Super-Twisting Based Sliding Mode Control of Drum Boiler Energy Conversion Systems

Article *in* International Journal of Control · February 2021

DOI: 10.1080/00207179.2021.1884293

6 authors, including:

Yazan M. Alsmadi
Jordan University of Science and Technology
46 PUBLICATIONS **637** CITATIONS

SEE PROFILE

Imtiaz Ur Rehman
COMSATS University Islamabad
2 PUBLICATIONS **6** CITATIONS

SEE PROFILE

Ali Arshad
COMSATS University Islamabad
39 PUBLICATIONS **364** CITATIONS

SEE PROFILE

Isaac Chairez
Tecnológico de Monterrey
389 PUBLICATIONS **3,206** CITATIONS

SEE PROFILE

ARTICLE TEMPLATE

Super-Twisting Based Sliding Mode Control of Drum Boiler Energy Conversion Systems

Yazan M. Alsmadi[a], Imtiaz Ur Rehman[b], Ali A. Uppal[b], Vadim Utkin[c], Isaac Chairez[d] and Muhammed Ibbini[a]

[a] Electrical Engineering Department, Jordan University of Science and Technology, Irbid, Jordan; [b]Department of Electrical and Computer Engineering, COMSATS University Isamabad, Islamabad, Pakistan; [c]Electrical and Computer Engineering Department, The Ohio State University, Columbus, OH, USA; [d]UPIBI-Instituto Politecnico Nacional Mexico City, Mexico

ARTICLE HISTORY
Compiled February 17, 2021

ABSTRACT
A drum boiler is the most critical part of power generation plants. The control of highly nonlinear, multiple input and multiple output drum boiler system (DBS) is a challenging task. The efficiency of a DBS can be increased by maintaining a desired water level and pressure of the drum. In this work, a robust and finite time convergent super-twisting sliding mode algorithm is exploited to design output feedback controllers for the control-oriented model of the DBS, which maintain a desired water level and pressure of the drum. To make the model-based control possible, the unknown states of the DBS are estimated using a gain-scheduled Utkin observer (GSUO). A rigorous mathematical analysis has been included to show that the closed loop system is locally stable. The simulation results show that the super-twisting sliding mode controllers (STSMCs) yield the required performance even in the presence of parametric uncertainty, process and measurement and process noises, and external disturbance. To make a fair comparison, a quantitative analysis is also carried out for STSMC and PI controllers. The comparison shows that both the controllers consume same control energy, however, STSMC yields better performance, in terms of error convergence and speed of the response.

KEYWORDS
Drum boiler system, super twisting sliding mode control, gain-scheduled Utkin observer, energy conversion systems.

1. Introduction

As the energy demand is increasing in the modern world, power is being generated in different ways. A drum boiler is one of the fundamental components of a power plant, which converts water in to steam. For this purpose boiler needs heat energy, which can be obtained either by burning fossil fuels or by converting nuclear energy into heat, cf. (Sunil et al., 2017). The schematic of a typical drum boiler system (DBS) is shown in Fig. 1. The fans are used to recruit the hot gases produced in the furnace of the boiler. These hot gases travel through and absorb by the economizer, re-heater

CONTACT Vadim Utkin. Email: utkin.2@osu.edu

tubes, water-wall tubes, air preheater and super-heater tubes. The unabsorbed heat is diffused in the surrounding environment.

The working of a drum boiler system (DBS) is explained as follows. First of all, the water coming from the feed water pump enters the economizer section, where its temperature is raised by the heat absorbed by the economizer. The heated water flows into a steam drum from where it is transferred to the downcomer section. It then passes through a section of tubes known as water-wall where the change of phase takes place. The steam produced along with some moisture content again re-enters into the steam drum. The steam is purified from moisture by using super heater. The super-heated steam is then supplied to the turbine inlet. After the first turbine stage the temperature drops, so a good technique to increase the power plant efficiency is to bypass the steam completely and add more heat. This process is known as reheating, which is carried out by heat exchanger or re-heater, cf. (Molloy, 1997).

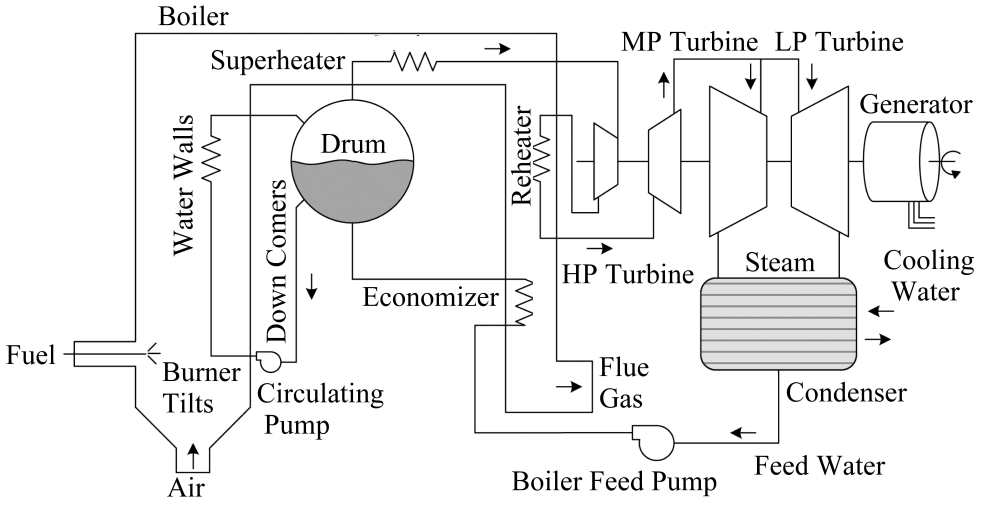

Figure 1. Schematic of Drum Boiler System (Naghizadeh et al., 2011)

In order to study the dynamics of a DBS, the researchers have developed various mathematical models, cf. (Åström and Eklund, 1972; Pellegrinetti and Bentsman, 1996). The performance of a DBS can be improved if the water level and pressure of the drum remains at a desired level. This task can be accomplished by designing a feedback controller, which automatically manipulates the flow rates of water and fuel. In the subsequent paragraph, the literature regarding mathematical modeling and control of a DBS is presented.

In (Tan et al., 2004), a control-oriented model of DBS is proposed, which has two inputs, control valve and fuel flow rate, and two outputs are pressure and power of the boiler and turbine, respectively. A model-based PID controller is designed for the DBS to improve its performance. In (Keadtipod and Banjerdpongchai, 2016) an LTI model of DBS is considered. The main contribution is the improved efficiency of the DBS by designing a multi-loop control scheme. A PID controller is used in the inner loop, whereas, a model predictive controller (MPC) is employed in the outer loop. Moreover, it is concluded that the cascaded control scheme yields better performance as compared to the standalone MPC design. (Tan et al., 2002) propose a robust controller for a boiler system using the model in (Keadtipod and Banjerdpongchai, 2016). A loop-shaping based H_∞ controller is designed to maintain pressure, water and steam

temperature at the desired level. Moreover, the designed controller is approximated by a simpler PI controller, which exhibits better performance. In (Swarnakar et al., 2008) a robust, observer based controller is designed using linear matrix inequalities (LMIs) for the first principles based model proposed in (Åström and Bell, 2000). In (Damiran et al., 2016; Horalek and Imsland, 2011) linear and nonlinear MPCs are designed for the model proposed in (Pellegrinetti and Bentsman, 1996). In both cases the control objective is to maintain a desired water level and pressure of the drum. As the model given in (Pellegrinetti and Bentsman, 1996) is highly nonlinear, therefore, the performance of nonlinear MPC is better as compared to its linear counterpart. In (Mahmoodi Takaghaj et al., 2014), a neuro-adaptive controller is designed for a waste to energy boiler, the unknown states are estimated using a nonlinear observer. It has been shown that the performance of the designed technique is better as compared to the conventional PI controller. However, the outputs and the states of the observer deviate from the reference values and original states, respectively. In (Fu et al., 2004; Pellegrinetti and Bentsman, 1994) H_∞ and robust PI controllers are designed for the model proposed in (Pellegrinetti and Bentsman, 1996). In (Dimeo and Lee, 1995), genetic algorithm (GA) is used to design a state feedback and PI controllers for the nonlinear boiler model developed by (Åström and Eklund, 1972). The results of the designed controllers are compared with the standard LQR controller. It has been demonstrated that the GA/PI algorithm yields good tracking performance at the cost of oscillatory response due to integral action. Whereas, the GA/LQR gives good performance but results in a finite steady state error. In literature various control techniques have been implemented on DBS model proposed by (Åström and Eklund, 1972) to enhance its reliability and performance. These include a guaranteed cost nonlinear state feedback tracking control using linear matrix inequalities (LMIs) approach proposed by (Wu et al., 2010), a nonlinear state feedback controller by (Lu et al., 2010) and a multivariable robust adaptive sliding mode control by (Ghabraei et al., 2015).

Most of the literature cited in the above paragraph does not consider the effect of parametric uncertainties, process and measurement noises and external disturbance on the performance of the closed loop system. These practical issues can affect the performance of the designed controllers. Therefore, it is required to design such a controller for the DBS which can efficiently maintain a desired pressure and a water level of the drum. Moreover, the controller should exhibit satisfactory performance in the presence of modeling imperfections and external disturbance.

In this paper, the nonlinear control oriented model of (Pellegrinetti and Bentsman, 1996) is employed to design two decentralized super twisting (ST) based sliding mode controllers (SMCs) for the DBS, which maintain the water level and pressure of the drum at the desired values. Apart from the property of robustness against parametric uncertainties and external disturbances offered by the conventional SMC, the super twisting sliding mode control (STSMC) also exhibits finite time convergence and yields a continuous control input (Utkin, 2013). Moreover, as the STSMC belongs to the class of higher order SMC, therefore, it also results in reduced chattering (LEVANT, 1993).

In order to make the model based control possible, the unknown states of the DBS are reconstructed using a gain scheduled Utkin observer (GSUO). The design of the GSUO is based on the quasi-linear decomposition of the nonlinear control-oriented model. After the establishment of sliding mode, the zero dynamics of the DBS is also derived and its boundedness is proved. To make a fair comparison, the performance of the STSMC algorithm is compared with the conventional proportional-integral (PI) controller. Simulation results show that super twisting and PI controllers consume similar control energy, however, the STSMCs exhibit better tracking performance.

Moreover, STSMC algorithm show robustness against an input disturbance, measurement and process noises and parametric uncertainties.

This paper is organized as follows: The control oriented model of the DBS is explained in Section 2, the statement of the problem is presented in Section 3. The STSMCs and the GSUO are designed in Sections 4 and 4.5, respectively. The control implementation scheme is discussed in Section 5, the simulation results are presented in Section 6 and the article is concluded in Section 7.

2. Control oriented model of drum boiler system

The mathematical model of Gordon and Joseph, cf. Pellegrinetti and Bentsman (1996) has been adapted for the model-based control of the DBS. The model proposed in Pellegrinetti and Bentsman (1996) is simplified by Fu et al. (2004) for designing a control system to maintain desired values of water level and drum pressure, which is also the aim of this research work. The reduced order model of the DBS is given by following set of equations

$$\begin{aligned}
\dot{x}_1 &= a_{11}x_3x_1^{9/8} + a_{12}u_1 - a_{13}u_2 + a_{14},\\
\dot{x}_2 &= a_{31}x_1 - a_{32}x_3x_1 - a_{33}u_2,\\
\dot{x}_3 &= -a_{41}x_3 + a_{42}u_1 + a_{43} + n_1 + w_d,
\end{aligned} \tag{1}$$

where $x^T = \begin{bmatrix} x_1 & x_2 & x_3 \end{bmatrix}$ are states of the DBS, $u^T = \begin{bmatrix} u_1 & u_2 \end{bmatrix}$ are normalized control inputs and $w_d \in \Re^+$ is a constant input disturbance specifying the load level, n_1 is colored noise and a_{ij} are constant model parameters given in Table 1.

The measured outputs of the DBS are given as

$$\begin{aligned}
y_1 &= a_{51}x_1 + n_2,\\
y_2 &= a_{70}x_1 + a_{71}x_2 + a_{72}x_3x_1 + a_{73}u_2 + a_{74}u_1\\
&\quad + \frac{\big(a_{75}x_1 + a_{76}\big)\big(1 - a_{77}x_2\big)}{x_2\big(x_1 + a_{78}\big)} + a_{79} + n_3.
\end{aligned} \tag{2}$$

The states, inputs and outputs of the DBS are defined in Table 2. The color noises n_1, n_2 and n_3 are given by following transfer functions

$$\begin{aligned}
\frac{n_1}{w_1} &= \frac{0.003s + 0.003}{s + 0.0075},\\
\frac{n_2}{w_2} &= \frac{0.75s + 0.1}{s + 0.01},\\
\frac{n_3}{w_3} &= \frac{0.105s + 0.038}{s + 0.010},
\end{aligned} \tag{3}$$

where $w_k, k = 1, 2, 3$ represents white noise.

Table 1. Nominal model parameters

a_{11}=−0.00478	a_{12}=0.280	a_{13}=0.01348
a_{14}=0.02493	a_{31}=0.00533176	a_{32}=0.02519504
a_{33}=0.7317058	a_{41}=0.04	a_{42}=0.029988
a_{43}=0.018088	a_{51}=14.2144	a_{70}=−0.1048569
a_{71}=0.15479	a_{72}=0.4954961	a_{73}=−0.207974
a_{74}=1.2720	a_{75}=−324212.7805	a_{76}=−99556.24778
a_{77}=0.0011850	a_{78}=−1704.50476	a_{79}=−103.7351

Table 2. List of symbols

Symbol	**Description**	**Units**
x_1	Drum pressure	kgf/cm^2
x_2	System fluid density	kg/m^3
x_3	Position of valve	—
y_1	Drum pressure	PSI
y_2	Water level	in
u_1	Fuel flow rate	—
u_2	Water flow rate	—

3. Problem statement

The objective of this paper is to design a robust control system that utilizes the inputs u_1 and u_2 to keep y_1 and y_2 at the prescribed levels. The control problem should be solved in the presence of process and measurement noises, external disturbance w_d and parametric uncertainties.

In order to achieve the above control objective two STSMCs are designed for the DBS in the subsequent section.

4. Control design

4.1. Design of the sliding surfaces

Prior to the controller design, a rigorous study is carried out for the DBS. It has been observed that the drum pressure y_1 is more sensitive to the fuel flow rate u_1. Whereas, the water flow rate u_2 has greater impact on the water level of the drum y_2 as compared to y_1. Therefore, for controller design, the DBS is conceptually divided into two subsystems: one for controlling y_1 through u_1 and the other for regulating y_2 using u_2. The cross coupling terms in the subsystems are considered as input disturbances. The sliding variables for maintaining a desired constant pressure y_{1_d} and a constant water level y_{2_d} are σ_1 and σ_2, respectively, which are characterized as

$$\begin{aligned} \sigma_1 &= \dot{e_1} + \lambda e_1 + \zeta \int_0^t e_1 d\tau, \\ \sigma_2 &= e_2, \end{aligned} \tag{4}$$

where $e_1 = y_1 - y_{1_d}$, $e_2 = y_2 - y_{2_d}$ and $\lambda, \zeta \in \Re^+$ are design parameters.

A PID type sliding variable has been proposed for y_1 to improve the performance during the sliding mode. On the other hand, the choice of σ_2 is motivated by a rigorous simulation study, which shows that the best response of y_2 is obtained if the sliding variable is simply the error between actual and desired values of the drum level y_2. Therefore, the sliding variable for regulating y_2 is simply the error between actual and the desired water levels.

It is pertinent to mention that the transfer functions for the colored noises in (3) are ignored during the controller design. However, these noises are considered during the simulations of the closed loop system to test the performance of the designed controllers.

4.2. Dynamics of the sliding surfaces

The time derivatives of the sliding variables can be written as

$$\begin{aligned} \dot{\sigma}_1 &= \phi_1(t,x) + \xi_{11}(t,x)u_1 + \xi_{12}(t,x)u_2 + a_{12}\dot{u}_1, \\ \dot{\sigma}_2 &= \phi_2(t,x) + \xi_{21}(t,x)u_1 + \xi_{22}(t,x)u_2 + a_{73}\dot{u}_2, \end{aligned} \tag{5}$$

where $||\phi_i|| \leq \Phi_i \in \Re^+$ and $i = 1, 2$. By using (1), (2) and (4) the functions ϕ_1 and ϕ_2 are obtained as given by the following equations

$$\begin{aligned} \phi_1 = &\left(a_{11}x_3x_1^{9/8} + a_{14}\right)\left(\lambda a_{51} + \frac{9}{8}a_{51}a_{11}x_3x_1^{1/8}\right) \\ &+a_{51}a_{11}x_1^{9/8}\left(-a_{41}x_3 + a_{43}\right) + \zeta\left(a_{51}x_1 - y_{1_d}\right) \\ \phi_2 = &\,\theta\left(a_{70} + a_{72}x_3 + \frac{a_{75}\left(1 - a_{77}x_2\right)}{\chi} - \frac{\left(a_{75}x_1 + a_{76}\right)\left(1 - a_{77}x_2\right)}{\varpi}\right), \\ &+\vartheta\left(a_{71} - \frac{a_{77}\left(a_{75}x_1 + a_{76}\right)}{\chi} - \frac{\left(a_{75}x_1 + a_{76}\right)\left(1 - a_{77}x_2\right)}{\chi x_2}\right), \\ &+a_{72}x_1\left(-a_{41}x_3 + a_{42}u_1 + a_{43}\right), \end{aligned} \tag{6}$$

where the parameters θ, ϑ, χ and ϖ are characterized as

$$\begin{aligned} \theta &= a_{11}x_3x_1^{9/8} + a_{14}, \\ \vartheta &= a_{31}x_1 - a_{32}x_3x_1, \\ \chi &= x_2\left(x_1 + a_{78}\right), \\ \varpi &= x_2\left(x_1 + a_{78}\right)^2. \end{aligned}$$

The input associated terms ξ_{11}, ξ_{12}, ξ_{21} and ξ_{22} are:

$$
\begin{aligned}
\xi_{11} &= \left(\lambda a_{51} + \frac{9}{8} a_{51} a_{11} x_3 x_1^{1/8}\right) a_{12} + a_{51} a_{11} x_1^{9/8} a_{42} \\
\xi_{12} &= -\left(\lambda a_{51} + \frac{9}{8} a_{51} a_{11} x_3 x_1^{1/8}\right) a_{13} \\
\xi_{21} &= a_{12}\left(a_{70} + a_{72} x_3 + \frac{a_{75}\left(1 - a_{77} x_2\right)}{\chi} - \frac{\left(a_{75} x_1 + a_{76}\right)\left(1 - a_{77} x_2\right)}{\varpi}\right) \\
\xi_{22} &= -a_{13}\left(a_{70} + a_{72} x_3 + \frac{a_{75}\left(1 - a_{77} x_2\right)}{\chi} - \frac{\left(a_{75} x_1 + a_{76}\right)\left(1 - a_{77} x_2\right)}{\varpi}\right) - \\
& \quad a_{33}\left(a_{71} - \frac{a_{77}\left(a_{75} x_1 + a_{76}\right)}{\chi} - \frac{\left(a_{75} x_1 + a_{76}\right)\left(1 - a_{77} x_2\right)}{\chi x_2}\right)
\end{aligned} \tag{7}
$$

In order to obtain the upper bounds on the functions ϕ_1 and ϕ_2, the DBS in a secure operating range leads to calculate the bounds for such parameters. Then, comprehensive simulation studies are carried out to yield $\Phi_1 = 0$ and $\Phi_2 = 0.08$.

4.3. The controller design and the stability analysis

As the DBS given by (1) and (2) depends linearly on the control and its derivative, the STSMC laws for maintaining the desired water level and drum pressure can be expressed as

$$
\begin{aligned}
\dot{u}_1 &= -\frac{\xi_{11}(t,x)}{a_{12}} u_1 - \frac{\xi_{12}(t,x)}{a_{12}} u_2 - \frac{\phi_1(t,x)}{a_{12}} + v_1 \\
\dot{u}_2 &= -\frac{\xi_{22}(t,x)}{a_{73}} u_2 - \frac{\xi_{21}(t,x)}{a_{73}} u_1 - \frac{\phi_2(t,x)}{a_{73}} + v_2
\end{aligned} \tag{8}
$$

where

$$
v_i = -\alpha_i |\sigma_i|^{0.5} \operatorname{sign}(\sigma_i) - \beta_i \int_0^t \operatorname{sign}(\sigma_i) d\tau, \tag{9}
$$

The controller gains α_i and β_i are given as

$$
\begin{aligned}
&\beta_1 > \frac{\Phi_1}{a_{12}}, \quad \beta_2 > \frac{\Phi_2}{a_{73}}, \\
&\alpha_1^2 \geq \frac{4\Phi_1 a_{12}(\beta_1 + \Phi_1)}{a_{12}^3(\beta_1 - \Phi_1)}, \quad \alpha_2^2 \geq \frac{4\Phi_2 a_{73}(\beta_2 + \Phi_2)}{a_{73}^3(\beta_2 - \Phi_2)}.
\end{aligned} \tag{10}
$$

The substitution of the proposed controller on the dynamics of the sliding surfaces (5) leads to

$$
\dot{\sigma}_i = -\alpha_i |\sigma_i|^{0.5} \operatorname{sign}(\sigma_i) - \beta_i \int_0^t \operatorname{sign}(\sigma_i) d\tau \tag{11}
$$

Defining $\sigma_{i1} = \sigma_i$ and $\sigma_{i2} = \dot{\sigma}_i$, then (11) can be transformed to

$$\begin{aligned} \dot{\sigma}_{i1} &= \sigma_{i2} - \alpha_i |\sigma_{i1}|^{0.5} \operatorname{sign}(\sigma_{i1}) \\ \dot{\sigma}_{i2} &= -\beta_i \operatorname{sign}(\sigma_{i1}) \end{aligned} \tag{12}$$

According to the results presented in (Angulo et al., 2013), the selection of the gains presented in (10) leads to prove that the origin is a finite time stable equilibrium point of (12) for both sliding surfaces. The proof is complete.

The values of the controller gains represent sufficient condition for the finite time convergence to the sliding manifold. Due to the STSMC algorithm according to LEVANT (1993), the sliding modes are confined in the manifolds $\sigma_1 = \dot{\sigma}_1 = 0$ and $\sigma_2 = \dot{\sigma}_2 = 0$, which result in reduced chattering, cf. LEVANT (1993). Moreover, the errors e_1 and e_2 converge in finite time, cf. Utkin (2013).

The STSMC design in (9) is only valid if the zero dynamics of the DBS is bounded. Therefore, the stability of the zero dynamics is explored in the following subsection.

4.4. Stability of the zero dynamics

After the sliding mode has been established, $\sigma_1 = \sigma_2 = 0$, and by using $\operatorname{sign}(0) = 0$ in (9), $u_1 \to U_1$ and $u_2 \to U_2$, where $U_1, U_2 \in \Re^+$. Now, by ignoring n_i and substituting $y_1 = y_{1_d}$ (the desired pressure is constant) in (2) the steady state value of x_1 is $X_1 = \frac{y_{1_d}}{a_{51}}$. As the DBS has two outputs, therefore, the zero dynamics of the DBS is only comprised of x_3, whose dynamics is given in (1), which can be re-written as

$$\dot{x}_3 = -a_{41} x_3 + \Gamma, \tag{13}$$

where $\Gamma = a_{43} + a_{42} U_1 + w_d$ is a constant.

The solution of the linear non-homogeneous differential equation in (13) is given as

$$x_3(t) = X_3 + \Big(x_3(t_0) - X_3\Big) \exp^{\left(-(t-t_0)a_{41}\right)}, \tag{14}$$

where $X_3 = \frac{\Gamma}{a_{41}}$.

As a_{41} is positive (cf. Table 1), therefore, $x_3 \to X_3$ and X_2 (the steady state value of x_2) can be evaluated by substituting X_1, X_3, U_1 and U_2 in (2). Hence, the zero dynamics of the DBS is bounded. Now the effect of colored noises n_i on the stability of the closed system needs to be investigated. It can be seen in (3) that all the transfer functions between the colored and white noises are stable. Therefore, n_i will oscillate and stay bounded. The amplitude of the oscillations is determined by the variance of the white noise w_i. Consequently, the zero dynamics is stable, even in the presence of n_i and the controller design is valid.

4.5. Control gain calculation using the gain scheduled Utkin observer

The formal realization of the controller design, requires to estimate the unknown states, because the time derivative of the tracking error for the drum pressure $\dot{e}_1 = a_{51}(a_{11} x_3 x_1^{9/8} + a_{12} u_1 - a_{13} u_2 + a_{14})$ in (4) is a function of x_1 and x_3. Moreover, the

estimates of unknown states are also required to compute the gains of the designed controllers, cf. (6).

Notice that the drum boiler system is forward complete. This characteristic allows to design the observer independently of the controller because of they both converge in finite time robustly. This condition simplifies the design of the controller and allows to handle the observer design as follows.

In this work, the states of the DBS are estimated using a GSUO, whose design is explained in this section. The nonlinear control-oriented model of the DBS in (1) can be re-written in a control affine form, i.e.,

$$\dot{x} = f(x) + b_1 u + b_2 w_d, \tag{15}$$

where $x \in \Re^3$ is the state vector, $u \in \Re^2$ is the control input vector, $w_d \in \Re^+$ is an input disturbance, and $f \in \Re^3$, $b_1 \in \Re^{3\times 2}$ and $b_2 \in \Re^3$ are smooth vector fields given by

$$\begin{aligned} f(x) &= \begin{bmatrix} a_{11}x_3 x_1^{9/8} + a_{14} \\ a_{31} - a_{32}x_3 x_1 \\ -a_{41}x_3 \end{bmatrix}, \\ b_1 &= \begin{bmatrix} a_{12} & -a_{13} \\ 0 & -a_{33} \\ a_{42} & 0 \end{bmatrix}, \\ b_2 &= \begin{bmatrix} 0 & 0 & 1 \end{bmatrix}^T. \end{aligned} \tag{16}$$

Similarly, (2) can be re-written as

$$y = h(x) + du, \tag{17}$$

where $y \in \Re^2$ $h \in \Re^2$ and $d \in \Re^{2\times 2}$. Moreover, smooth vector field h and d are given as

$$\begin{aligned} h(x) &= \begin{bmatrix} a_{5,1}x_1 \\ x_1(\mathcal{C}_1 + a_{72}x_3 - \mathcal{C}_2 x_2) + x_2(a_{71} - \mathcal{C}_3) + \mathcal{C}_4 \end{bmatrix}, \\ d &= \begin{bmatrix} 0 & 0 \\ a_{74} & a_{73} \end{bmatrix}, \end{aligned} \tag{18}$$

where $\mathcal{C}_1 = a_{70} + a_{75}$, $\mathcal{C}_2 = a_{75}a_{77}$, $\mathcal{C}_3 = a_{76}a_{77}$ and $\mathcal{C}_4 = a_{76} + a_{77}$.

The design of the GSUO is based on the quasi-linear decomposition of 16, which is obtained by linearization of $f(x)$ and $h(x)$ using the method given in Teixeira and Zak (1999). The conventional linearization method, based on the first-order Taylor series approximation does not yield a good approximation of the nonlinear function for any arbitrary operating point or even for a non-zero equilibrium point. The step by step method for linearizing $f(x)$ is discussed in detail. In Teixeira and Zak (1999), this issue is resolved by formulating a constrained convex optimization problem, which aims to construct a quasi-linear model in x, u and w_d that gives an exact decomposition of (16) at any arbitrary operating point x_{opt}, i.e.,

$$\dot{x} = f(x) + b_1 u + b_2 w_d = A(x)x + b_1 u + b_2 w_d. \tag{19}$$

Similarly, for any arbitrary x_{opt}, (19) can be written as

$$\dot{x}_{opt} = f(x_{opt}) + b_1 u + b_2 w_d = A(x_{opt})x_{opt} + b_1 u + b_2 w_d. \tag{20}$$

Now the task is to find such a state-dependent matrix $A(x) \in \Re^{3\times 3}$, such that in the vicinity of x_{opt}

$$f(x) = A(x)x \; and \; f(x_{opt}) = A(x_{opt})x_{opt}. \tag{21}$$

Let the set $\{r_i,\ i = 1, 2, 3\}$ represents the columns of $A(x)$, then (21) takes the form

$$f_i(x) = r_i^T(x)x, \tag{22}$$
$$f_i(x_{opt}) = r_i^T(x_{opt})x_{opt}. \tag{23}$$

where the index $i = 1, 2, 3$.

By expanding $f_i(x)$ in (22) around x_{opt}, using Taylor's series expansion, and neglecting the higher order terms results in

$$f_i(x) = f_i(x_{opt})\nabla^T f_i(x_{opt})(x - x_{opt}) = r_i^T(x)x, \tag{24}$$

where $\nabla^T f_i(x) \in \Re^3$ is the gradient of f_i evaluated at x. Using the result in (23), (24) takes the form

$$\nabla^T f_i(x_{opt})(x - x_{opt}) = r_i^T(x_{opt})(x - x_{opt}), \tag{25}$$

Where x is arbitrary but "close" to x_{opt}. Now to find r_i, a constrained optimization problem is formulated as

$$\begin{aligned} &\min_{r_i} \mathcal{E} = \frac{1}{2} \left\| \nabla f_i(x_{opt}) - r_i(x_{opt}) \right\|_2^2, \\ &\text{such that } f_i(x_{opt}) = r_i^T(x_{opt})x_{opt}. \end{aligned} \tag{26}$$

The problem in (26) is convex, which means that the first-order necessary condition for a minimum of $\mathcal{E}$ is also sufficient. The first order conditions for (26) are

$$\nabla_{r_i}\mathcal{E} + \lambda\nabla_{r_i}(r_i^T x_{opt} - f_i(x_{opt})) = 0, \tag{27}$$
$$r_i^T x_{opt} = f_i(x_{opt}), \tag{28}$$

where λ is the Lagrange multiplier. The differentiation of (27) gives

$$r_i - \nabla f_i(x_{opt}) + \lambda x_{opt} = 0. \tag{29}$$

Here we consider the case when $x_{opt} \neq 0$. Now pre-multiplying (29) by x_{opt} and substituting (28) in the resulting equation yields

$$\lambda = \frac{x_i^T \nabla f_i(x_{opt}) - f_i(x_{opt})}{\left\| x_{opt} \right\|^2}. \tag{30}$$

Finally, r_i is obtained by substituting (30) in (29)

$$r_i = \nabla f_i(x_{opt}) + \frac{f_i(x_{opt}) - x_i^T \nabla f_i(x_{opt})}{\|x_{opt}\|^2} x_{opt}, \qquad x_{opt} \neq 0. \tag{31}$$

Similarly, $h(x)$ in (17) is linearized to obtain the $C(x) \in \Re^{2\times 3}$ matrix. The ith column of $C(x)$ is given as

$$c_i = \nabla h_i(x_{opt}) + \frac{h_i(x_{opt}) - x_i^T \nabla h_i(x_{opt})}{||x_{opt}||^2} x_{opt}, \qquad x_{opt} \neq 0. \tag{32}$$

Here, it is pertinent to mention that if the operating point is the origin of the state space, i.e., $x_{opt} = 0$, then the task of determining matrices $A(x)$ and $C(x)$ reduces to finding the jacobian of the nonlinear functions $f(x)$ and $h(x)$ along the system's states, respectively.

Now, the quasi-linear decomposition of (15) and (17) is characterized by

$$\begin{aligned} \dot{x} &= A(x)x + b_1 u + b_2 w_d \\ y &= C(x)x + du, \end{aligned} \tag{33}$$

where the matrices b_1, b_2 and d are already defined in (16) and (17). Whereas, using the results in (31) and (32), $A(x)$ and $C(x)$ are given by

$$\begin{aligned} A(x) &= \begin{bmatrix} | & | & | \\ r_1 & r_2 & r_3 \\ | & | & | \end{bmatrix}, \\ C(x) &= \begin{bmatrix} | & | & | \\ c_1 & c_2 & c_3 \\ | & | & | \end{bmatrix}. \end{aligned} \tag{34}$$

The ansatz of the corresponding gain-scheduled Utkin observer (GSUO) is

$$\dot{\hat{x}} = A(\hat{x})\hat{x} + b_1 u + L(\hat{x})\,\mathrm{sign}\big(y - C(\hat{x})\hat{x}\big), \tag{35}$$

where $L(\hat{x}) \in \Re^{3\times 2}$ is the observer gain matrix, computed using the LQR method. It is important to note that the structure of the observer is similar to the one proposed by Drakunov and Utkin (1995), however, in this work $L(\hat{x})$ is computed using the state dependent matrices $A(x)$ and $C(x)$, therefore, the value of $L(\hat{x})$ is adapted according to the operating point. The LQR method minimizes the cost of the following quadratic function

$$J = \int_0^t \big(\hat{x}^T Q \hat{x} + y^T R y\big) d\tau, \tag{36}$$

where $Q \in \Re^{3\times 3}$ and $R \in \Re^{2\times 2}$ are weighting matrices, given by

$$Q = diag(\Pi_1^2; \Pi_2^2; \Pi_3^2;),$$
$$R = diag(\Omega_1^2; \Omega_2^2), \tag{37}$$

where the constants $\Pi_i, i \in \{1, 2, 3\}$ and $\Omega_j, j \in \{1, 2\}$ are chosen to be

$$\Pi_i = \varphi \left(\frac{\pi_i}{\hat{x}_{i,\,max}^2} \right) \quad and \quad \Omega_j = \left(\frac{\omega_i}{e_{y,j\,max}^2} \right), \tag{38}$$

where $e_y = y - \hat{y}$ is the measurement error. The values of π_i and ω_j are chosen to facilitate the state estimation and convergence of measurement error, respectively. Furthermore, the relative weighting between Q (state reconstruction) and R (measurement error convergence) is set by changing the value of φ. With the change in $\hat{x}_{opt}$ the matrices $A(\hat{x})$ and $C(\hat{x})$ change, hence the matrix $L(\hat{x})$ adapts accordingly to ensure that the matrix $A(\hat{x}_{opt}) - L(\hat{x}_{opt})C(\hat{x}_{opt})$ remains Hurwitz, i.e., its eigen values lie in the open left half of the complex plane for any arbitrary $\hat{x} = \hat{x}_{opt} \neq 0$.

The stability of both the controller and the observer implies that the closed loop system is stable. However, it is important to mention that the stability is only local, as it is only valid in $\mathcal{S} = \{x | x = x_{opt}\}$.

5. Control implementation scheme

The overall implementation of the STSMCs and GSUO is illustrated in Fig. 2. In order to emulate the practical scenario, the dynamics of the control valves is also included in the implementation. The control valves are modeled with first order transfer functions as

$$\frac{\eta_i}{u_i} = \frac{1}{\mathcal{T}_i s + 1}, \tag{39}$$

where s is the Laplace variable, $\mathcal{T}_i$ is the time constant and η_i represents the actual input of the DBS. The saturation blocks are incorporated to limit the control inputs between their legitimate values, i.e., $\eta_1, \eta_2 \in [0, 1]$.

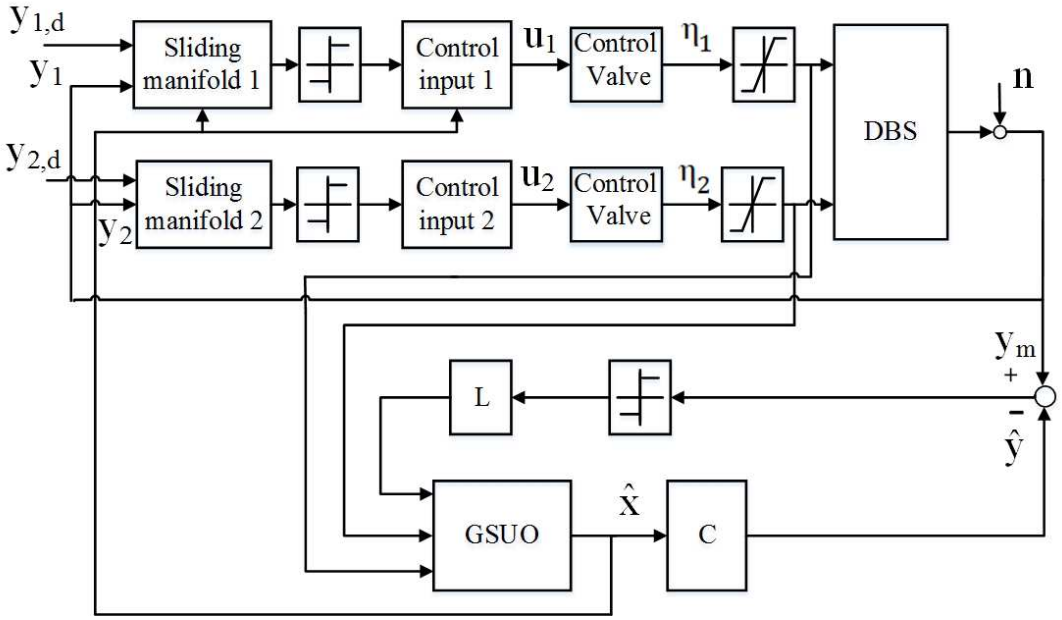

Figure 2. Control scheme

6. Results and discussions

This section presents the simulation results of the DBS along with the STSMCs and GSUO. The simulations are performed using MATLAB/Simulink. Furthermore, the performance of the designed controllers are compared with the conventional PI controllers. To present a real time scenario, following practical considerations are considered:

- A fixed step ode solver, with a step size of 0.1 s is selected to solve the closed loop system. The time constant $\mathcal{T} = 0.6$ s for both the control valves given in (39).
- By substituting $\Phi_1 = 0$ and $\Phi_2 = 0.08$ in (10) and conducting extensive simulations, following gains are selected for the controllers: $\alpha_1 = 0.7$, $\alpha_2 = 0.7$, $\beta_1 = 0.01$ and $\beta_2 = 0.01$. Moreover, $\lambda = 7$ and $\zeta = 7.25$ are selected for the desired sliding mode dynamics: $\sigma_1 = \dot{\sigma_1} = 0$, cf. (4).
- The colored noises n_1, n_2 and n_3 given in the mathematical model of DBS in (1) and (2) are considered during the simulations to study their effect on the performance of the STSMCs and the GSUO. These noises can be classified in to two groups: the process noise, n_1 and the measurement noises, n_2 and n_3. These noises are generated by stimulating the transfer functions in (3) with additive white Gaussian noises w_i, with zero mean and the variance of 0.0025.
- To assess the robustness of the control and estimation schemes, the effect of parametric uncertainties is also introduced in the DBS. The model parameters which are subjected to 5% parametric uncertainties are listed in Table 3.
- A constant non-vanishing input disturbance $w_d = 3 \times 10^{-3}$ (load level, cf. (1)) is also considered in the simulations to study the robustness of the closed loop system.
- The desired value for the drum pressure, $y_{1_d} = 320$ kgf/cm^2, whereas, it is desired to keep the water level at zero, i.e., $y_{2_d} = 0$ in.

- The structure of the PI controllers used for the comparison is given as

$$u_{PI_i} = -K_{p_i} e_i(t) - K_{I_i} \int_0^t e_i(t) d\tau \tag{40}$$

where K_{p_i} and K_{I_i} are proportional and integral gains, respectively, $e_i = y_i - y_{i_d}$, $i \in \{1, 2\}$ represents the tracking error for the pressure and water level of the DBS, respectively.

Table 3. Parameters subjected to perturbations

Parameters	Nominal Value	Perturbed Value
a_{42}	0.029988	0.0314874
a_{43}	0.018088	0.017183
a_{70}	−0.1048569	−0.0996140
a_{77}	0.0011850	0.0012442
a_{79}	−103.7351	−98.5483

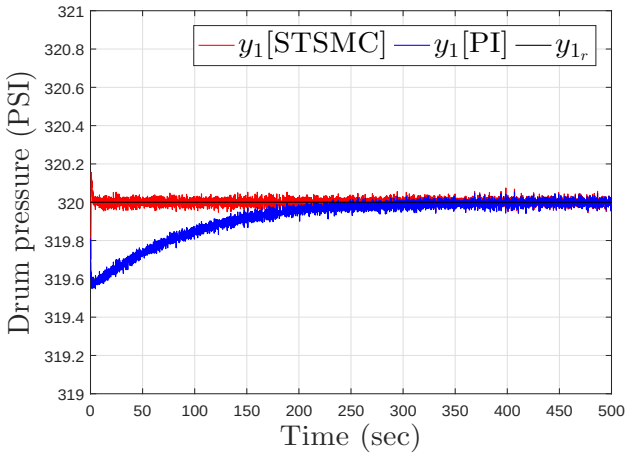

Figure 3. Drum pressure with time.

When the closed loop operation starts, the controllers drag the outputs to their desired values in finite time, which can be seen in the Figs. 3 and 4, respectively. The corresponding controller efforts are depicted in Figs. 5 and 6. It can be seen that even in the presence of modeling imperfections like parametric uncertainties, measurement and process noises and the external matched disturbance w_d, the controllers successfully drag the outputs to their desired levels.

The sliding surfaces for the STSMCs are depicted in Figs. 7 and 8. It can be seen that when the sliding mode occurs in the manifold $\sigma_1 = \dot{\sigma_1} = 0$, then the STSMC drags e_1 to 0 and eventually y_1 reaches its desired value. On the other hand for the regulation of water level of the drum, the sliding variable is simply the tracking error, i.e., $\sigma_2 = e_2$.

In order to make a fair comparison between the controllers, the proportional and

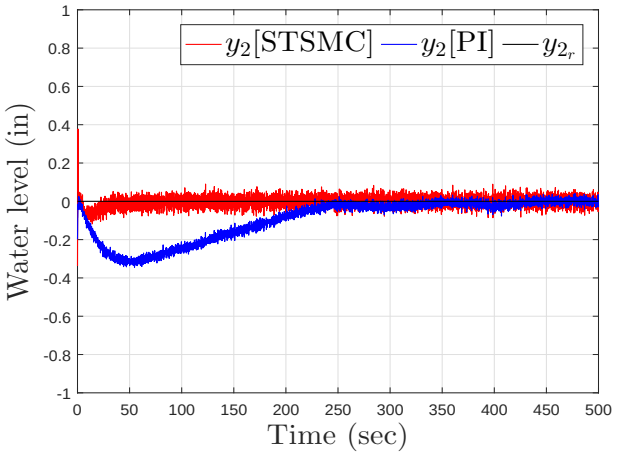

Figure 4. Water level of the drum with time.

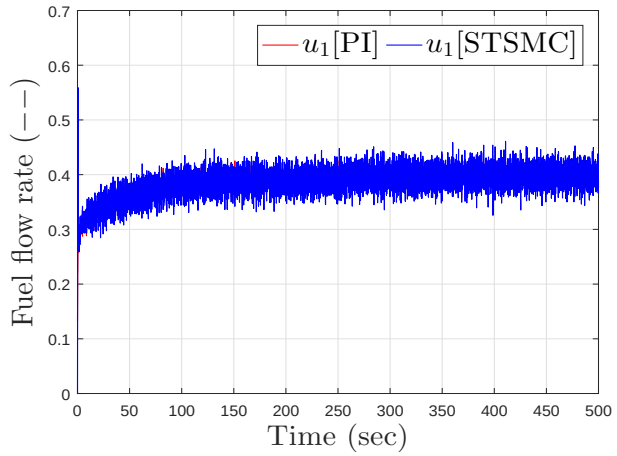

Figure 5. Normalized fuel flow rate input to DBS.

integral gains of both STSMCs and PI controllers are identical, therefore, $K_{P_1} = \alpha_1 = 0.7$, $K_{P_2} = \alpha_2 = 0.7$, $K_{I_1} = \beta_1 = 0.01$ and $K_{I_2} = \beta_2 = 0.01$.

The simulation results demonstrate that the performance of the STSMCs is better as compared to the PI controllers, as the designed controllers bring the outputs to their desired values in finite time. A detailed quantitative comparison is also made between the two control schemes by computing the root mean squared error (RMSE) for both the outputs, which is given as

$$\text{RMSE}_i = \sqrt{\frac{1}{N}\sum_{j=1}^{N} e_i^2(j)}, \quad e_i(j) = y_i(j) - y_{i_d}(j), \tag{41}$$

where N are the number of samples and $i \in \{1, 2\}$ is the index for the RMSE value of the output i. Another performance index, is the measure of the utilization of the control energy, which is quantified by calculating the average power for the control

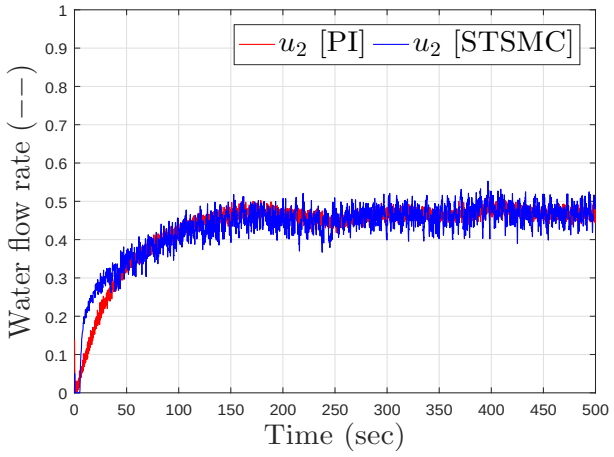

Figure 6. Time profile of normalized water flow rate.

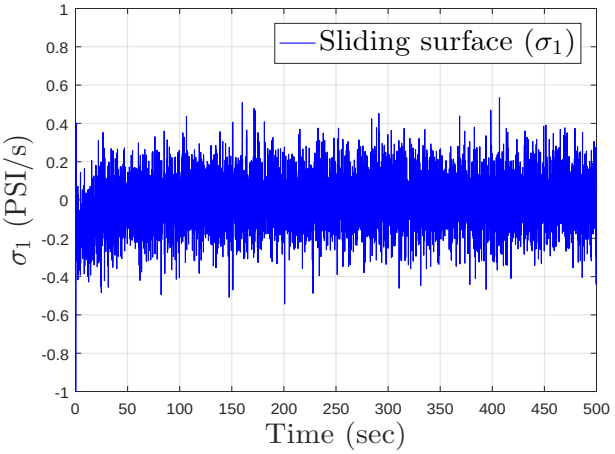

Figure 7. Sliding variable for the drum pressure control.

signals generated by the controllers. The expression for the average power $\mathrm{P_{avg}}$ of the control signal takes the form

$$\mathrm{P_{avg_k}} = \frac{1}{N}\sum_{j=1}^{N} u_k^2(j), \tag{42}$$

where the index $k \in \{1, 2\}$ refers to the $\mathrm{P_{avg}}$ of the control input k. The statistics for the RMSE and the $\mathrm{P_{avg}}$ for both the tracking errors and the control inputs are given in Table 4. The results clearly show that both the control schemes consume same control energy, however, the performance of the STSMC is better as compared to its counterpart.

To study the performance of the estimator, it is mandatory to initialize both the DBS and the GSUO with different initial conditions. Therefore, the initial state vector for the boiler plant is $x(0) = \begin{bmatrix} 22.5 & 621.17 & 0.694 \end{bmatrix}^T$, whereas, the GSUO is initialized

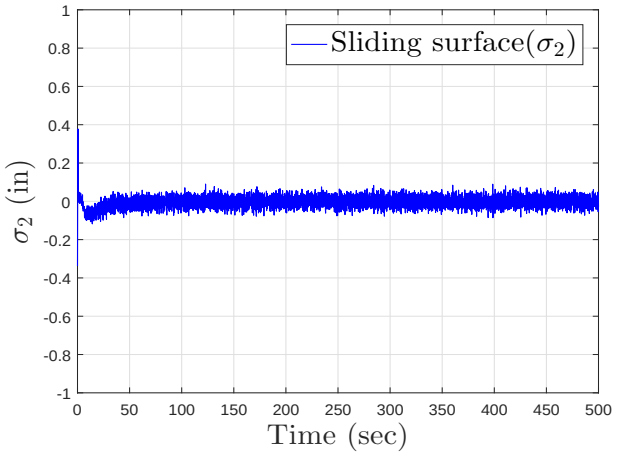

Figure 8. Sliding variable for the drum water level control.

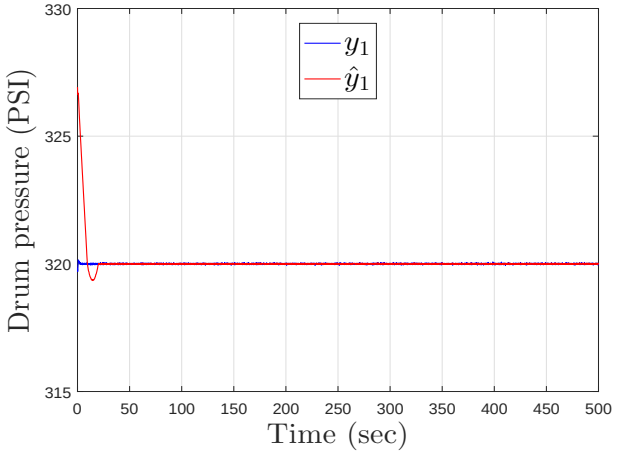

Figure 9. Measured and estimated drum pressures.

with $\hat{x}(0) = \begin{bmatrix}23 & 623 & 0.9\end{bmatrix}^T$. The measured and estimated outputs are shown in Figs. 9 and 10. The results of the state reconstruction are demonstrated in Figs. 11, 12 and 13. As it has been already mentioned in Section 4.5 that an LQR method is used to design the observer gain matrix L. Therefore, the matrices Q and R are selected in such a way to yield good state reconstruction and measurement error convergence. It can be seen form the results that true and the estimated states are in good agreement. The state reconstruction is almost perfect for x_1 and x_2, however, a little deviation can be observed for x_3. The modeling uncertainties and the external unknown disturbance w_d create deviation in the estimate of x_3 and y_2.

Moreover, the results in Figs. 11, 12 and 13 also conform with the analytical findings regarding the zero dynamics of the DBS in Section 4. It can be seen from the simulation results that the estimated states stay bounded during the closed loop operation of the DBS.

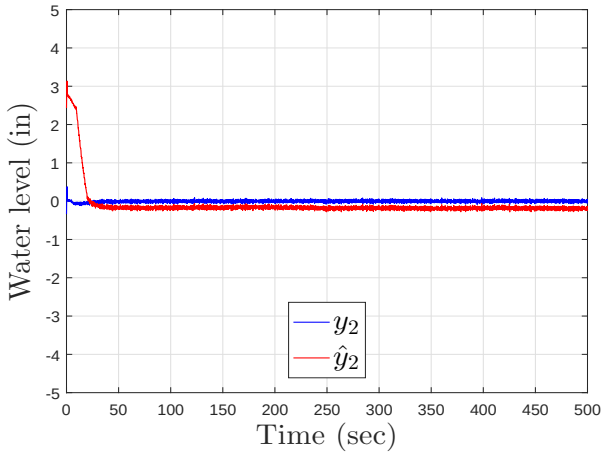

Figure 10. Measured and estimated water levels of the drum.

Table 4. Comparison of PI and STSMC

Figure of Merit	**PI Controller**	**STSMC**
RMSE_1	0.1361	0.0198
RMSE_2	0.1416	0.0321
P_{avg_1}	0.1495	0.1502
P_{avg_2}	0.1915	0.1901

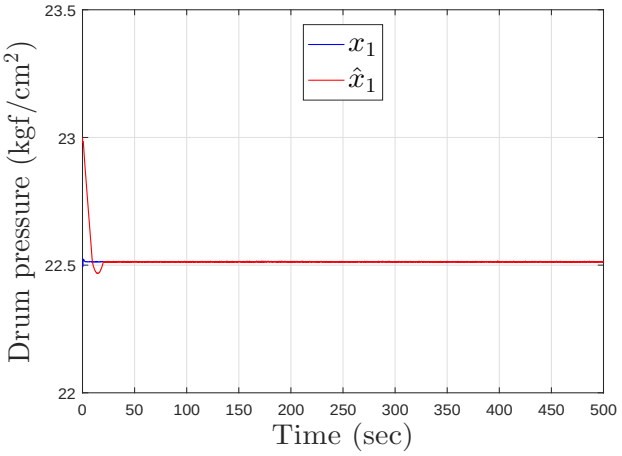

Figure 11. Actual and estimated drum pressures.

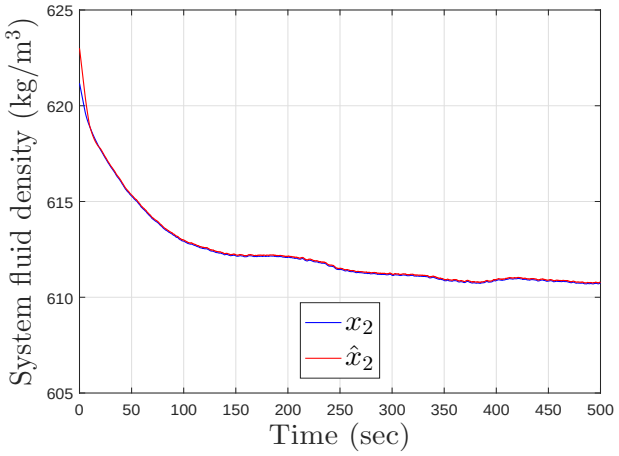

Figure 12. Actual and estimated system fluid densities.

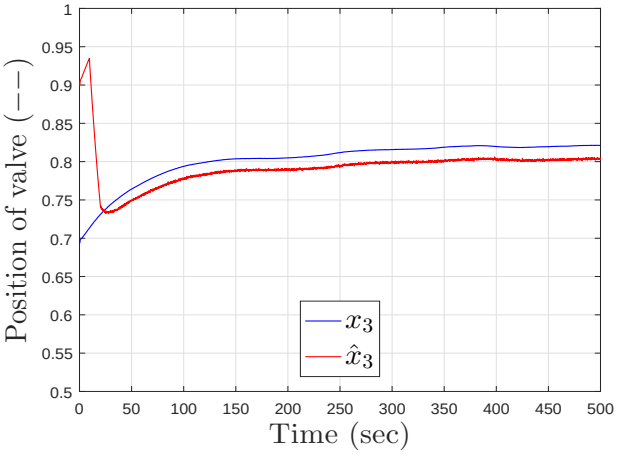

Figure 13. Actual and estimated positions of valve.

7. Conclusion

In this paper, model based STSMCs are designed for the control-oriented model of the DBS system. The controllers maintain the pressure and water level of the drum at the desired values. The task of the feedback controller design is made possible by estimating the unknown states of the system using the GSUO. The design of the GSUO is based on the quasi-linear decomposition of the DBS. In order to make the state estimation robust, the observer gain matrix is designed using an LQR method. The state dependent matrices in the quasi-linear decomposition enable the gain-scheduling of the observer gain matrix. The simulation results show the effectiveness of the STSMCs and GSUO to achieve the desired control task in the presence of external disturbance, measurement and process noises and parametric uncertainties. A comprehensive quantitative comparison is also made between the super-twisting and the PI controllers, which demonstrate that the STMC algorithm exhibit better performance as compared to its counterpart.

The focus of the current research is to integrate the DBS with a steam turbine, and deploy the system in a micro grid configuration along with other distributed energy resources.

References

Angulo, M. T., Moreno, J. A., and Fridman, L. (2013). Robust exact uniformly convergent arbitrary order differentiator. *Automatica*, 49(8):2489–2495.

Åström, K. J. and Bell, R. D. (2000). Drum-boiler dynamics. *Automatica*, 36(3):363–378.

Åström, K. J. and Eklund, K. (1972). A simplified non-linear model of a drum boiler-turbine unit. *International Journal of Control*, 16(1):145–169.

Damiran, U., Fu, C., and Tan, W. (2016). Model predictive control of nonlinear drum boiler. In *Strategic Technology (IFOST), 2016 11th International Forum on*, pages 544–548. IEEE.

Dimeo, R. and Lee, K. Y. (1995). Boiler-turbine control system design using a genetic algorithm. *IEEE transactions on energy conversion*, 10(4):752–759.

Drakunov, S. and Utkin, V. (1995). Sliding mode observers. tutorial. In *Decision and Control, 1995., Proceedings of the 34th IEEE Conference on*, volume 4, pages 3376–3378. IEEE.

Fu, C., Liu, J., and Tan, W. (2004). Robust pi design for a benchmark nonlinear boiler. In *Control Conference, 2004. 5th Asian*, volume 1, pages 304–308. IEEE.

Ghabraei, S., Moradi, H., and Vossoughi, G. (2015). Multivariable robust adaptive sliding mode control of an industrial boiler–turbine in the presence of modeling imprecisions and external disturbances: A comparison with type-i servo controller. *ISA transactions*, 58:398–408.

Horalek, R. and Imsland, L. (2011). Nonlinear model predictive control of a benchmark nonlinear boiler. In *Information, Communication and Automation Technologies (ICAT), 2011 XXIII International Symposium on*, pages 1–6. IEEE.

Keadtipod, P. and Banjerdpongchai, D. (2016). Design of supervisory cascade model predictive control for industrial boilers. In *Automatic Control Conference (CACS), 2016 International*, pages 122–125. IEEE.

LEVANT, A. (1993). Sliding order and sliding accuracy in sliding mode control. *International Journal of Control*, 58(6):1247–1263.

Lu, Z., Lin, W., Feng, G., and Wan, F. (2010). A study of nonlinear control schemes for a boiler-turbine unit. *IFAC Proceedings Volumes*, 43(14):1368–1373.

Mahmoodi Takaghaj, S., Macnab, C., Westwick, D., and Boiko, I. (2014). Neural-adaptive control and nonlinear observer for waste-to-energy boilers. *Asian Journal of Control*, 16(5):1323–1333.

Molloy, B. (1997). *Modelling and predictive control of a drum-type boiler*. PhD thesis, Dublin City University.

Naghizadeh, R. A., Vahidi, B., and Bank Tavakoli, M. R. (2011). Estimating the parameters of dynamic model of drum type boilers using heat balance data as an educational procedure. *IEEE Transactions on Power Systems*, 26(2):775–782.

Pellegrinetti, G. and Bentsman, J. (1994). H∞ controller design for boilers. *International Journal of Robust and Nonlinear Control*, 4(5):645–671.

Pellegrinetti, G. and Bentsman, J. (1996). Nonlinear control oriented boiler modeling-a benchmark problem for controller design. *IEEE transactions on control systems technology*, 4(1):57–64.

Sunil, P., Barve, J., and Nataraj, P. (2017). Mathematical modeling, simulation and validation of a boiler drum: Some investigations. *Energy*, 126:312–325.

Swarnakar, A., Marquez, H. J., and Chen, T. (2008). A new scheme on robust observer-based control design for interconnected systems with application to an industrial utility boiler. *IEEE Transactions on control systems technology*, 16(3):539–547.

Tan, W., Liu, J., Fang, F., and Chen, Y. (2004). Tuning of pid controllers for boiler-turbine units. *ISA transactions*, 43(4):571–583.

Tan, W., Marquez, H. J., and Chen, T. (2002). Multivariable robust controller design for a boiler system. *IEEE Transactions on Control Systems Technology*, 10(5):735–742.

Teixeira, M. C. and Zak, S. H. (1999). Stabilizing controller design for uncertain nonlinear systems using fuzzy models. *IEEE Transactions on Fuzzy systems*, 7(2):133–142.

Utkin, V. (2013). On convergence time and disturbance rejection of super-twisting control. *IEEE Transactions on Automatic Control*, 58(8).

Wu, J., Nguang, S. K., Shen, J., Liu, G. J., and Li, Y. G. (2010). Guaranteed cost nonlinear tracking control of a boiler-turbine unit: an lmi approach. *International Journal of Systems Science*, 41(7):889–895.